

1 Real-time measurement of cellular bioenergetics in fully differentiated human nasal epithelial
2 cells grown at air-liquid-interface.

3

4 Emily Mavin¹, Bernard Verdon², Sean Carrie³, Vinciane Saint-Criq², Jason Powell¹, Christian
5 A. Kuttruff⁴, Chris Ward^{1,2}, James P. Garnett^{1,5*#}, Satomi Miwa^{2*}

6 * Equal contributions made. # Corresponding author.

7

8 1 - Institute of Cellular Medicine, Newcastle University, Newcastle upon Tyne, NE2 4HH, UK.

9 2 - Institute for Cell and Molecular Biosciences, Newcastle University, Newcastle upon Tyne,
10 NE2 4HH, UK

11 3 – Institute of Health and Society, Newcastle University, Newcastle upon Tyne, NE2 4HH.
12 UK.

13 4 - Medicinal Chemistry, Boehringer Ingelheim Pharma GmbH & Co. KG, Birkendorfer
14 Straße 65, 88397 Biberach an der Riss, Germany

15 5 - Immunology and Respiratory Diseases Research, Boehringer Ingelheim Pharma GmbH
16 & Co. KG, 8840 Biberach an der Riss, Germany

17

18 Author contributions:

19 EM performed research, data analysis and prepared the manuscript.

20 BV performed research and commented on manuscript.

21 SC, VSC, JP and CK contributed to data interpretation, commented on manuscript.

22 CW and JG designed the study and prepared the manuscript

23 SM performed research, data analysis, designed the study and prepared the manuscript

24

25 Running head: Metabolism in airway epithelial cells

26 Correspondence to Dr James Garnett: james.garnett@boehringer-ingenheim.com

27

28 **Abstract**

29 Shifts in cellular metabolic phenotypes have the potential to cause disease-driving processes
30 in respiratory disease. The respiratory epithelium is particularly susceptible to metabolic shifts
31 in disease, but our understanding of these processes are limited by the incompatibility of the
32 technology required to measure metabolism in real-time with the cell culture platforms used to
33 generate differentiated respiratory epithelial cell types. Thus to date, our understanding of
34 respiratory epithelial metabolism has been restricted to that of basal epithelial cells in
35 submerged culture, or via indirect endpoint metabolomics readouts in lung tissue. Here we
36 present a novel methodology using the widely available Seahorse Analyzer platform to monitor
37 real-time changes in the cellular metabolism of fully differentiated primary human airway
38 epithelial cells grown at air-liquid interface (ALI). We show increased glycolytic, but not
39 mitochondrial, ATP production rates in response to physiologically relevant increases in
40 glucose availability. We also show that pharmacological inhibition of lactate dehydrogenase is
41 able to reduce glucose-induced shifts towards aerobic glycolysis. This method is timely given
42 the recent advances in our understanding of new respiratory epithelial subtypes that can only
43 be observed *in vitro* through culture at ALI and will open new avenues to measure real-time
44 metabolic changes in healthy and diseased respiratory epithelium, and in turn the potential for
45 the development of novel therapeutics targeting metabolic-driven disease phenotypes.

46

47 **Introduction**

48 Metabolic phenotypes are influenced by a number of genetic and environmental factors
49 including gender, age, diet, microbiome, exercise, hormones and medication. Each unique
50 combination, and therefore unique metabolic phenotype, can determine the disease risk of an
51 individual. This is of particular importance in respiratory disease research; recent studies have
52 demonstrated that altered metabolic phenotypes can modulate disease-driving cellular
53 processes prevalent in the pathologies of chronic lung diseases, such as cellular proliferation,
54 differentiation, apoptosis, autophagy, senescence and inflammation (12, 28, 29). Despite the
55 high metabolic activity of the lung, with glucose metabolism in particular surpassing that of
56 many other organs (12), our understanding of metabolic dysfunction as a driver or
57 consequence of respiratory disease pathology is limited.

58 Much of the lung's metabolic activity occurs in the epithelium where cells have dense apical
59 concentrations of mitochondria and carry out energy demanding processes such as
60 mucin/surfactant production and mucociliary clearance (27). The respiratory epithelium
61 provides a barrier to prevent nutrients entering the respiratory tract from the interstitium/blood
62 and through tight control of glucose transport the glucose concentration in the airway is
63 maintained at 3-20-fold lower than in plasma (6). In healthy airway epithelium, glucose is
64 rapidly processed by hexokinase-dependent and -independent metabolic pathways to
65 maintain low intracellular glucose concentrations (1). However, airway glucose concentrations
66 are elevated in respiratory disease and hyperglycaemia, which is associated with increased
67 risk of respiratory infection (2, 18, 19). Thus understanding the metabolic processes underlying
68 lung metabolite homeostasis in health and disease could identify new therapeutic targets for
69 the treatment of lung infections. The Seahorse platform is an excellent tool for interrogating
70 cellular metabolism, measuring oxygen consumption rate (OCR) and extracellular acidification
71 rate (ECAR), in real time. Recent studies modelling the human airway epithelium have utilised
72 this technology to show how mitochondrial dysfunction, caused by cigarettes and e-cigarettes,
73 might contribute to the pathology of lung disease (3, 23) as well as investigating how infection

74 influences epithelial cell metabolism (13). While these studies all provide key information on
75 airway cell metabolism, the data is all generated using epithelial cells grown in submerged
76 cultures. Accordingly, a methodological development to monitor real time metabolic changes
77 of fully differentiated airway epithelial cells, under a range of conditions, would be of particular
78 benefit to the field of respiratory research.

79 Since Whitcutt *et al* (25) first described a method to grow airway epithelial cells at an air-liquid-
80 interface (ALI) this has become widely used to investigate epithelial barrier function. ALI
81 cultures are an excellent research resource as once the cells fully differentiate they have a
82 range of features which are not present in undifferentiated cells (25). They form polarised
83 barriers with characteristic epithelial ion transport properties and contain a heterogeneous cell
84 population of secretory and ciliated cells which only become apparent *in vitro* when the cells
85 are maintained at ALI. Recent single cell profiling has further demonstrated the heterogeneity
86 of ALI cultures at a molecular level and allowed the authors to identify a rare and novel
87 epithelial cell type, the pulmonary ionocyte (20). This highlights the importance of studying a
88 heterogeneous mixture of differentiated cells, which makes our exploration of epithelial
89 metabolism in ALI cultures particularly timely.

90 There are very few studies which have attempted to measure cellular metabolism in
91 differentiated airway epithelial cells, and the only report which we are aware required the in-
92 house manufacture of cell culture equipment (27), which is beyond the resources of many
93 researchers. We describe a novel method utilising the Seahorse XF24 Analyzer platform to
94 monitor real time changes in the cellular bioenergetics of human airway epithelial cells fully
95 differentiated at an air-liquid-interface. We describe a simple protocol, predicated on
96 inexpensive and widely available equipment.

97

98

99 **Methods**

100 *Sample source*

101 We obtained approval for the collection of clinical waste material obtained during routine nasal
102 surgical procedures [Newcastle Biobank application NB-169, Research Ethics Committee
103 Reference 17/NE/0361]. Written informed consent was obtained from all participants.

104 *Epithelial cell culture at air-liquid interface (ALI)*

105 Primary human airway epithelial cells were isolated from clinical waste material obtained
106 during routine nasal surgical procedures. Chopped sections of epithelial tissue (approx. 1mm³)
107 were cultured in PneumaCult™-Ex Plus Medium (STEMCELL Technologies) for 7-9 days in
108 Type I collagen coated flasks (Purecol 30 µg/ml). P1 cells were then transferred onto collagen
109 coated 0.4µm pore size transwells (Costar) at 150,000 cells/cm². Once the cells were fully
110 confluent (2-4 days) apical media was removed and basolateral media was switched to
111 PneumaCult™-ALI version 2 custom medium (STEMCELL Technologies) and the cells were
112 maintained at ALI until fully differentiated (25). Barrier integrity of ALI cultures was monitored
113 by measuring trans-epithelial electrical resistance (EVOM 2, World Precision Instruments) and
114 ion channel function assessed using Ussing chamber short circuit current measurements.
115 Transwells were routinely fixed with 2% glutaraldehyde for TEM/SEM (Newcastle University
116 Electron Microscopy Research Services) and 4% PFA for H&E staining (NHS Cellular
117 Pathology, RVI Newcastle).

118 *Seahorse XF24 Analyzer*

119 All reagents were obtained from Sigma, unless stated otherwise. Apical washes, with pre-
120 warmed PBS, of the ALI cultures were carried out 24 hours prior to all seahorse experiments.
121 Sections of ALI cultures on Transwells were cut from the membrane using a 3 mm punch
122 biopsy (Kai Medical). These were carefully loaded into a seahorse islet capture plate (Agilent
123 Technologies) and held in place with the islet capture grid (Figure 2). Wells were loaded with

124 450 μ l experimental media (DMEM without NaHCO_3 , glucose or phenol red (Sigma),
125 supplemented with 1 mM D-glucose and 2 mM L-glutamine, pH 7.4 at 37°C). The plate was
126 incubated at 37°C without CO_2 while the cartridge was loaded and calibrated in XF24
127 Seahorse Analyzer (Agilent).

128 Cellular energetics for ATP production rates by mitochondrial oxidative phosphorylation and
129 glycolysis were calculated by using the OCR and ECAR (16). Un-buffered medium enables
130 the Seahorse Analyzer to accurately detect changes in acidification rates of the medium, as
131 lactate secretion associated with glycolysis causes an acidification of the medium. Changes
132 in OCR, after sequential inhibition of different stages of the electron transport chain, are used
133 to measure mitochondrial ATP production (16). Oligomycin inhibits ATP synthase, thus
134 oligomycin-induced changes in OCR reflect the oxygen consumption due to mitochondrial
135 ATP production, which is used to calculate the mitochondrial ATP production rates. Carbonyl
136 cyanide-4-(trifluoromethoxy)phenylhydrazone (FCCP) is an uncoupler, hence stimulating
137 electron transport chain and increasing OCR. Rotenone and Antimycin A, complex I and
138 complex III inhibitors respectively, block electron transport activity and hence mitochondrial
139 OCR and the OCR in the presence of them indicates non-mitochondrial respiration.

140 Injection ports for the cartridge were prepared in experimental buffer as follows. Injection port
141 A with 50 μ l of 1 mM, 14 mM or 140 mM D glucose (final concentrations to be 1 mM, 5 mM or
142 15 mM). Injection port B with 55 μ l of 50 $\mu\text{g}/\text{ml}$ oligomycin (final concentration 5 $\mu\text{g}/\text{ml}$ as
143 determined by titration shown in Figure 3). Injection port C with 60 μ l of 25 μM FCCP (final
144 concentration 2.5 μM , as determined by titration in Figure 3) and injection port D with 65 μ l of
145 25 μM Antimycin A and 5 μM Rotenone (final concentrations 2.5 μM and 0.5 μM respectively).
146 LDH5 inhibitor (synthesized according to the procedures described in patent WO 2015/140133
147 A1 (22)) was injected to a final concentration of 30 μM per well using DMSO vehicle control
148 where appropriate.

149 Cycles of; mix (2 minutes), wait (1 minute), measure (3 minutes) were used. After our
150 optimisation experiments we allowed 5 cycles for the cells to equilibrate, 7 cycles following

151 glucose injection, 11 cycles after oligomycin, 7 cycles after FCCP and 6 cycles following
152 antimycin A and Rotenone addition. For LDH5 inhibition assays we allowed 5 cycles for
153 equilibration, 7 cycles following glucose injection (port A), 13 cycles each following LHD5inh
154 injection (port B) and oligomycin (port C) with a final 7 cycles after antimycin A and Rotenone
155 (port D) injection.

156 Data analysis to calculate absolute ATP production rates was carried out using the methods
157 described by Mookerjee and Brand (16), taking into account the acidification rates due to
158 mitochondrial CO₂ production. All statistical analysis was carried out using GraphPad Prism
159 8.

160

161 **Results**

162 *Culture of ALI epithelial cells*

163 Primary human nasal epithelial cells were successfully grown at ALI to form fully differentiated
164 pseudostratified cultures (Figure 1A). Cilia were visible on the apical side (Figure 1A) and cells
165 were shown to contain a large number of apical mitochondria (Figure 1A). Our ALI cultures
166 showed electrophysiological polarisation and had characteristic ion transport systems as
167 measured in an Ussing system (Figure 1B). The initial short circuit current (I_{sc}) was completely
168 inhibited by amiloride (10 μM) indicating that this standing I_{sc} is carried by apical to basolateral
169 Na⁺ transport through apical epithelial sodium channels (ENaC). Further addition of forskolin
170 (10 μM) generated a positive I_{sc} which reached a plateau and was fully reversed with
171 CFTRinh-172, indicating apical Cl⁻ secretion via CFTR channels. Finally, addition of ATP (100
172 μM) generated a further positive I_{sc} (which decayed spontaneously). This is likely to be Cl⁻
173 efflux through apical Ca²⁺-activated Cl⁻ channels, activated by intracellular Ca²⁺ pulse (initiated
174 via ATP interaction with apical P2Y receptors).

175 *Seahorse Analyzer protocol optimisation*

176 Sections of membrane with cells attached were loaded into the seahorse islet plate and held
177 in place with the islet capture grid (Figure 2). We compared the oxygen consumption rate
178 (OCR) and extracellular acidification rate (ECAR) values when cells were loaded into the islet
179 plate with the cells either facing up or down. Significantly higher values for both OCR and
180 ECAR were obtained when cells were facing up (Figure 3A). Therefore, it was decided that for
181 all subsequent experiments disks of membrane would be loaded into the plate with the cells
182 facing up. Epithelial cells remained attached to the membrane throughout the experiment as
183 verified by visual inspection with brightfield microscopy.

184 Oligomycin concentrations ranging from 2.5-10 μM were tested. Each concentration was
185 sufficient to induce a decrease in OCR as mitochondrial ATP synthesis was inhibited. The
186 maximum change in OCR was seen in 5 μg/ml oligomycin without further decrease at 10 μg/ml

187 (Figure 3B), therefore 5 $\mu\text{g}/\text{ml}$ was selected for all subsequent experiments. The FCCP
188 concentration to induce maximum OCR was also determined (1.5–3.5 μM) and it was found
189 2.5 μM FCCP was sufficient to achieve the highest increase in OCR (Figure 3C). Importantly,
190 we found that it takes much longer for the pseudostratified cultures to achieve steady state
191 after glucose and drug injections than a simple monolayer of airway epithelial cells (7).

192 *ALI cultures at altered glucose concentrations*

193 Once experimental conditions had been optimised we tested the bioenergetic response of our
194 differentiated airway epithelial cells to altered glucose concentrations. We saw that following
195 addition of both 5 mM and 15 mM D-glucose levels of ECAR significantly increased, when
196 compared to 1 mM glucose while no changes were observed in OCRs in any of the glucose
197 concentrations (Figure 4A). Therefore, assuming mitochondrial CO_2 production rates also
198 remained the same, the changes in ECAR under these conditions would reflect the glycolysis
199 dependent medium acidification rate. Following addition of oligomycin the greatest decrease
200 in OCR was seen in the 1mM glucose samples.

201 Analysis of absolute ATP production rates showed that increasing the glucose concentration
202 causes a significant and progressive increase in ATP production by glycolysis from 252
203 pmol/min at 1 mM to 703 pmol/min at 5 mM and 952 pmol/min at 15 mM (Figure 4B). While
204 glycolytic ATP production rates increased with increasing levels of glucose, we saw that
205 mitochondrial (OXPHOS) ATP production rates significantly decreased from 798 pmol/min at
206 1 mM to 487 pmol/min at 5 mM and 362 pmol/min at 15 mM. There was no statistically
207 significant difference in OXPHOS ATP production rates between the 5 mM and 15 mM glucose
208 concentrations.

209 *Proof-of-concept: inhibition of LDH suppresses glucose-induced extracellular acidification*

210 Multiple chronic lung diseases, including COPD, CF and IPF are associated with elevated lung
211 lactate concentrations (26, 29), with the metabolic shifts towards glycolysis in the epithelium
212 being at least in part implicated in these observed changes (7). In order to suppress lactate

213 production by glycolysis in our fully differentiated ALI cultures we injected an inhibitor of lactate
214 dehydrogenase 5 (LDH5; Compound 408, Genentech; Figure 4C(22)). At all glucose
215 concentrations there was significant decrease in the maximum ECAR following LDH5 inhibitor
216 addition, with the greatest decrease at the highest concentration of 15 mM Glucose (Figure
217 4D). Therefore, we have demonstrated empirically that LDH5 inhibition indeed lowered
218 glycolytic activity of the cells.

219 **Discussion**

220 Our study presents a robust, practicable methodology that allows the metabolic
221 characterisation of differentiated primary human airway epithelial cell cultures using the widely
222 available Seahorse XF24 Analyzer platform. This allows multi-well measurements of real time
223 oxygen consumption and extracellular acidification rates in live cells, providing information on
224 glycolysis and mitochondrial function. To our knowledge this is the first time this has been
225 possible using commercially available equipment.

226 This study used primary nasal epithelial cells as an exemplar for methodology development,
227 due to their ability to replicate complex airway architecture *in vitro* (8). However, contrary to
228 the previously proposed airways model (21), it is clear that there are differences between the
229 upper and lower airway in their responses to disease relevant stimuli (4, 14) in addition to
230 alterations in the cellular composition of the airway epithelium down the tracheobronchial tree.
231 We suggest that our technique is broadly applicable to a range of airway cells grown on
232 standard transwell support systems, and thus could be used to compare the metabolic profile
233 of airway epithelial cells collected from different regions of the airway as well as comparisons
234 between health and disease.

235 This method also has transferability across other disease models where cells are grown on
236 Transwell inserts, in particular where there is also a close association between altered glucose
237 metabolism and disease risk (5, 15, 17). In principle this technique would open up additional
238 avenues for metabolic research beyond epithelial monocultures, such as co-cultures with
239 fibroblasts which also undergo significant metabolic shifts in disease-relevant conditions (22).

240 This would support development of novel therapeutic strategies for targeting epithelia-
241 fibroblast crosstalk in idiopathic pulmonary fibrosis and related fibrotic interstitial lung
242 diseases. Furthermore, because human variability is greater than that of animal models often
243 used to study a disease, individual *ex vivo* metabolic profiling of the airway using our methods
244 could provide vital information for personalized medicine (10). Such research could provide

245 much needed translational insights and facilitate the development of novel therapeutic
246 approaches.

247 We maintain that using ALI cultures is more physiologically relevant than using submerged
248 cells, indicating the need for a method to transfer ALI cultures into the Seahorse Analyzer
249 platform. The ALI cultures are highly differentiated, secretory, have motile cilia and therefore
250 are more likely to recapitulate the complex metabolic requirements of airway epithelial cells *in*
251 *vivo*. Basal epithelial cells, maintained in submerged culture, have a much lower rate of
252 glycolysis and mitochondrial respiration than those grown at ALI (27) and therefore are not
253 truly representative of *in vivo* airways. Furthermore, there are cell types which only become
254 apparent when cells are maintained at ALI (20). Thus, using this novel methodology the
255 Seahorse Analyzer is able to detect the integrated signal from the multiple cell types which
256 are present in ALI cultures. This allows for the *in vitro* modelling of a physiologically
257 heterogeneous whole airway epithelium rather than a single cell type.

258

259 We were able to show that in high, but physiologically relevant glucose conditions, ALI cultures
260 significantly increased the glycolysis dependent extracellular acidification rate. *In vivo* we
261 believe that this could result in an acidification of the airway surface liquid (ASL). Recent
262 research has suggested that the precise regulation of the ASL, in particular the pH, has a
263 critical role in the prevention of infection and disease pathology (9, 11, 24). Therefore the real
264 time monitoring of pH and glucose metabolism, using platforms such as the Seahorse
265 Analyzer, may be a key methodology for providing insights into the pathophysiology of airways
266 disease and for therapeutic development. This may be especially relevant in situations where
267 diabetes often represents an important comorbidity such as in cystic fibrosis, chronic
268 obstructive pulmonary disease, and bronchiectasis.

269

270 As well as providing novel information relevant to the pathophysiology of airways disease, our
271 study demonstrated proof of concept that cellular bioenergetics analysis of differentiated
272 epithelia may provide insights in pharmaceutical development. A range of pathophysiological

273 conditions including cancer and fibrotic lung diseases are thought to involve a reprogramming
274 of cellular metabolism, with skewing towards aerobic glycolysis, suggesting a potential
275 therapeutic target. We showed that the addition of a potent LDH5 inhibitor resulted in a dose
276 dependent reduction in extracellular acidification rate, consistent with a reduction in the
277 production of lactate from pyruvate (22). Our system therefore allowed the evaluation of a
278 novel compound in fully differentiated human cells, with the observed metabolic effects
279 predicted from its designed mode of action.

280

281 In conclusion, we present a novel method and supporting data to demonstrate that it is
282 possible to monitor the cellular metabolism in real time of fully ALI differentiated airway
283 epithelial cells. The method also allowed us to monitor cellular responses to altered glucose
284 concentrations, which may be relevant where diabetes and airway hyperglycemia can present
285 as comorbidities to chronic airways diseases. We also found that it is possible to manipulate
286 epithelial cell metabolism with a novel small molecule, indicating that this method may be
287 useful for evaluating future therapeutic drug candidates.

288

289

290

291 Funding: This work was funded by Medical Research Foundation (MRF Respiratory Diseases
292 Research Award to J. P. Garnett; Grant MRF-091-0001-RG-GARNE) and Boehringer
293 Ingelheim.

294

295

296 **Figure legends**

297 Figure 1. Nasal epithelial ALI culture characterisation. A) Hematoxylin and eosin stain, TEM
298 and SEM images of apical side of ALI culture. Scale bars indicate 10 μ m. B) Short circuit
299 current trace from Ussing chamber experiment of ALI culture showing conventional airway
300 epithelial responses to amiloride, forskolin, CFTR_{inh172} (all at 10 μ M) and ATP (100 μ M).
301 Chemical modulators were applied sequentially to the apical compartment of the Ussing
302 chamber. I_{SC} Short circuit current.

303 Figure 2. Schematic representation of ALI culture in Seahorse islet capture plate.

304 Figure 3. Protocol optimisation for Seahorse XF24 Analyzer. A) Comparison of ALI cultures
305 loaded into Islet capture plate with cells facing up or down in 10mM D-Glucose. Bar graphs
306 indicate basal levels of OCR and ECAR, before injection of any drugs. Error bars indicate
307 mean \pm SEM for 7-9 replicates and p values shown calculated by unpaired t test. B)
308 Oligomycin titration, left - OCR measurements normalised to last time point before addition
309 of oligomycin, right - area under the curve analysis of OCR, error bars indicate mean \pm SEM
310 for 5-7 replicates and p values calculated by one way ANOVA. C) FCCP titration, left OCR
311 normalised to last time point before addition of FCCP, right maximum OCR in each well
312 following addition of FCCP, error bars indicate mean \pm SEM for 5-6 replicates and p values
313 calculated by one way ANOVA.

314 Figure 4. Metabolic profiling of ALI cells at altered glucose concentrations. A) ECAR (left)
315 and OCR (right) normalised to last reading before addition of glucose. Data from 4-6 repeats
316 at each glucose concentration for 4 donors. Error bars indicate mean \pm SEM. B) Absolute
317 ATP production rates (left) and ATP production as a percentage of source, p values
318 calculated by 2 way ANOVA (4-6 repeats at each glucose concentration from 6 donors). C)
319 Dose dependent change in maximum ECAR before and after addition of LDH5inhibitor, all at
320 15 mM D glucose (3-5 repeats at each glucose concentration from 2 donors). D) Change in
321 maximum ECAR following addition of 30 μ M LDH5 inhibitor at 1 mM, 5 mM and 15 mM D

322 glucose, normalised to the average of control wells without inhibitor, p values calculated by
323 Mann-Whitney test (4-6 repeats at each glucose concentration from 3 donors).

324

325 **References**

- 326 1. **Bearham J, Garnett JP, Schroeder V, Biggart MGS, and Baines DL.** Effective glucose
327 metabolism maintains low intracellular glucose in airway epithelial cells after exposure to
328 hyperglycemia. *Am J Physiol Cell Physiol* 317: C983-C992, 2019.
- 329 2. **Brennan AL, Gyi KM, Wood DM, Johnson J, Holliman R, Baines DL, Philips BJ, Geddes DM,
330 Hodson ME, and Baker EH.** Airway glucose concentrations and effect on growth of respiratory
331 pathogens in cystic fibrosis. *Journal of cystic fibrosis : official journal of the European Cystic Fibrosis
332 Society* 6: 101-109, 2007.
- 333 3. **Clapp PW, Lavrich KS, van Heusden CA, Lazarowski ER, Carson JL, and Jaspers I.**
334 Cinnamaldehyde in flavored e-cigarette liquids temporarily suppresses bronchial epithelial cell ciliary
335 motility by dysregulation of mitochondrial function. *American journal of physiology Lung cellular and
336 molecular physiology* 316: L470-L486, 2019.
- 337 4. **Comer DM, Elborn JS, and Ennis M.** Comparison of nasal and bronchial epithelial cells
338 obtained from patients with COPD. *PLoS One* 7: e32924, 2012.
- 339 5. **De Bruijn KM, Arends LR, Hansen BE, Leeflang S, Ruiter R, and van Eijck CH.** Systematic
340 review and meta-analysis of the association between diabetes mellitus and incidence and mortality
341 in breast and colorectal cancer. *Br J Surg* 100: 1421-1429, 2013.
- 342 6. **Garnett JP, Baker EH, and Baines DL.** Sweet talk: insights into the nature and importance of
343 glucose transport in lung epithelium. *The European respiratory journal* 40: 1269-1276, 2012.
- 344 7. **Garnett JP, Kalsi KK, Sobotta M, Bearham J, Carr G, Powell J, Brodli M, Ward C, Tarran R,
345 and Baines DL.** Hyperglycaemia and *Pseudomonas aeruginosa* acidify cystic fibrosis airway surface
346 liquid by elevating epithelial monocarboxylate transporter 2 dependent lactate-H(+) secretion.
347 *Scientific reports* 6: 37955, 2016.
- 348 8. **Gianotti A, Delpiano L, and Caci E.** In vitro Methods for the Development and Analysis of
349 Human Primary Airway Epithelia. *Frontiers in pharmacology* 9: 1176, 2018.
- 350 9. **Haq IJ, Gray MA, Garnett JP, Ward C, and Brodli M.** Airway surface liquid homeostasis in
351 cystic fibrosis: pathophysiology and therapeutic targets. *Thorax* 71: 284-287, 2016.
- 352 10. **Holmes E, Wilson ID, and Nicholson JK.** Metabolic phenotyping in health and disease. *Cell*
353 134: 714-717, 2008.
- 354 11. **Kostikas K, Papatheodorou G, Ganas K, Psathakis K, Panagou P, and Loukides S.** pH in
355 expired breath condensate of patients with inflammatory airway diseases. *American journal of
356 respiratory and critical care medicine* 165: 1364-1370, 2002.
- 357 12. **Liu G, and Summer R.** Cellular Metabolism in Lung Health and Disease. *Annual review of
358 physiology* 81: 403-428, 2019.
- 359 13. **Maurice NM, Bedi B, Yuan Z, Goldberg JB, Koval M, Hart CM, and Sadikot RT.** *Pseudomonas*
360 *aeruginosa* Induced Host Epithelial Cell Mitochondrial Dysfunction. *Scientific reports* 9: 11929, 2019.
- 361 14. **Mihaylova VT, Kong Y, Fedorova O, Sharma L, Dela Cruz CS, Pyle AM, Iwasaki A, and
362 Foxman EF.** Regional Differences in Airway Epithelial Cells Reveal Tradeoff between Defense against
363 Oxidative Stress and Defense against Rhinovirus. *Cell Rep* 24: 3000-3007 e3003, 2018.
- 364 15. **Mills KT, Bellows CF, Hoffman AE, Kelly TN, and Gagliardi G.** Diabetes mellitus and
365 colorectal cancer prognosis: a meta-analysis. *Dis Colon Rectum* 56: 1304-1319, 2013.
- 366 16. **Mookerjee SA, and Brand MD.** Measurement and Analysis of Extracellular Acid Production
367 to Determine Glycolytic Rate. *J Vis Exp* e53464, 2015.
- 368 17. **Pang Y, Kartsonaki C, Guo Y, Bragg F, Yang L, Bian Z, Chen Y, Iona A, Millwood IY, Lv J, Yu C,
369 Chen J, Li L, Holmes MV, and Chen Z.** Diabetes, plasma glucose and incidence of pancreatic cancer: A
370 prospective study of 0.5 million Chinese adults and a meta-analysis of 22 cohort studies. *Int J Cancer*
371 140: 1781-1788, 2017.

- 372 18. **Philips BJ, Meguer JX, Redman J, and Baker EH.** Factors determining the appearance of
373 glucose in upper and lower respiratory tract secretions. *Intensive care medicine* 29: 2204-2210,
374 2003.
- 375 19. **Philips BJ, Redman J, Brennan A, Wood D, Holliman R, Baines D, and Baker EH.** Glucose in
376 bronchial aspirates increases the risk of respiratory MRSA in intubated patients. *Thorax* 60: 761-764,
377 2005.
- 378 20. **Plasschaert LW, Zilionis R, Choo-Wing R, Savova V, Knehr J, Roma G, Klein AM, and Jaffe
379 AB.** A single-cell atlas of the airway epithelium reveals the CFTR-rich pulmonary ionocyte. *Nature*
380 560: 377-381, 2018.
- 381 21. **Rimmer J, and Ruhno JW.** 6: Rhinitis and asthma: united airway disease. *Med J Aust* 185:
382 565-571, 2006.
- 383 22. **Schruf E, Schroeder V, Kuttruff CA, Weigle S, Krell M, Benz M, Bretschneider T, Holweg A,
384 Schuler M, Frick M, Nicklin P, Garnett JP, and Sobotta MC.** Human lung fibroblast-to-myofibroblast
385 transformation is not driven by an LDH5-dependent metabolic shift towards aerobic glycolysis.
386 *Respiratory research* 20: 87, 2019.
- 387 23. **Sundar IK, Maremanda KP, and Rahman I.** Mitochondrial dysfunction is associated with
388 Miro1 reduction in lung epithelial cells by cigarette smoke. *Toxicol Lett* 317: 92-101, 2019.
- 389 24. **Torres IM, Patankar YR, and Berwin B.** Acidosis exacerbates in vivo IL-1-dependent
390 inflammatory responses and neutrophil recruitment during pulmonary *Pseudomonas aeruginosa*
391 infection. *American journal of physiology Lung cellular and molecular physiology* 314: L225-L235,
392 2018.
- 393 25. **Whitcutt MJ, Adler KB, and Wu R.** A biphasic chamber system for maintaining polarity of
394 differentiation of cultured respiratory tract epithelial cells. *In Vitro Cell Dev Biol* 24: 420-428, 1988.
- 395 26. **Worlitzsch D, Meyer KC, and Doring G.** Lactate levels in airways of patients with cystic
396 fibrosis and idiopathic pulmonary fibrosis. *American journal of respiratory and critical care medicine*
397 188: 111, 2013.
- 398 27. **Xu W, Janocha AJ, Leahy RA, Klatte R, Dudzinski D, Mavrakis LA, Comhair SA, Lauer ME,
399 Cotton CU, and Erzurum SC.** A novel method for pulmonary research: assessment of bioenergetic
400 function at the air-liquid interface. *Redox biology* 2: 513-519, 2014.
- 401 28. **Zank DC, Bueno M, Mora AL, and Rojas M.** Idiopathic Pulmonary Fibrosis: Aging,
402 Mitochondrial Dysfunction, and Cellular Bioenergetics. *Frontiers in medicine* 5: 10, 2018.
- 403 29. **Zhao H, Dennery PA, and Yao H.** Metabolic reprogramming in the pathogenesis of chronic
404 lung diseases, including BPD, COPD, and pulmonary fibrosis. *American journal of physiology Lung
405 cellular and molecular physiology* 314: L544-L554, 2018.

406

Figure 1 – Nasal epithelial ALI culture characterisation

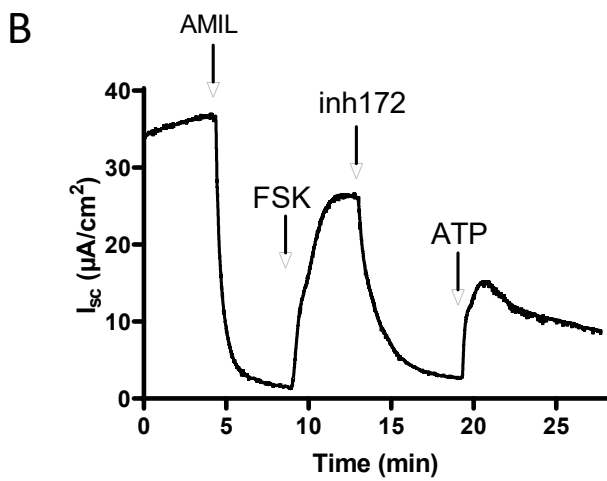
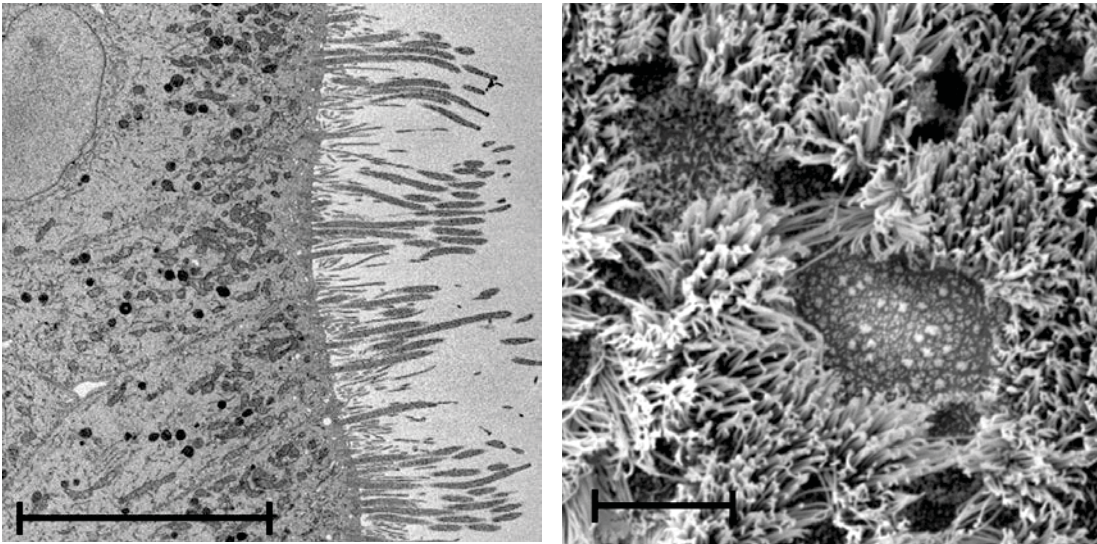
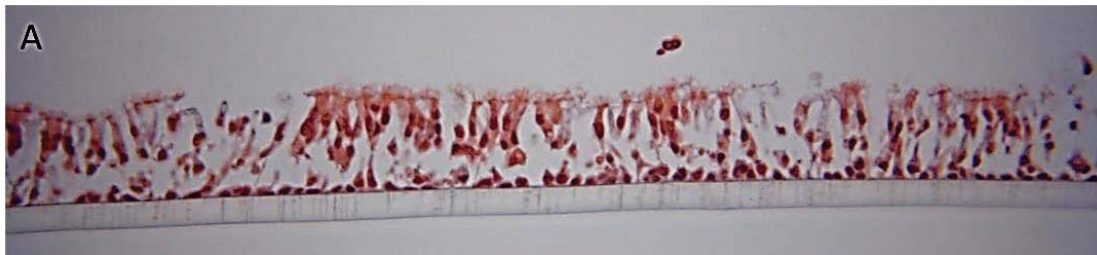


Figure 2 –ALI culture in seahorse plate

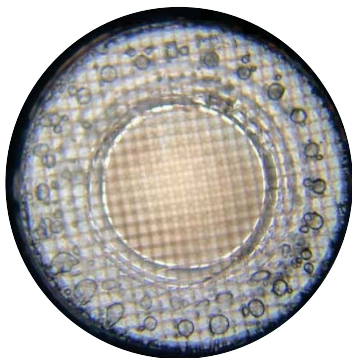
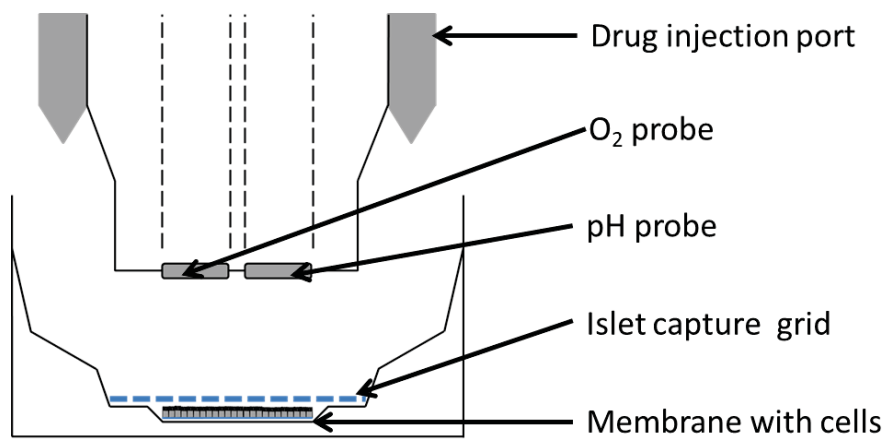


Figure 3 – Protocol optimisation

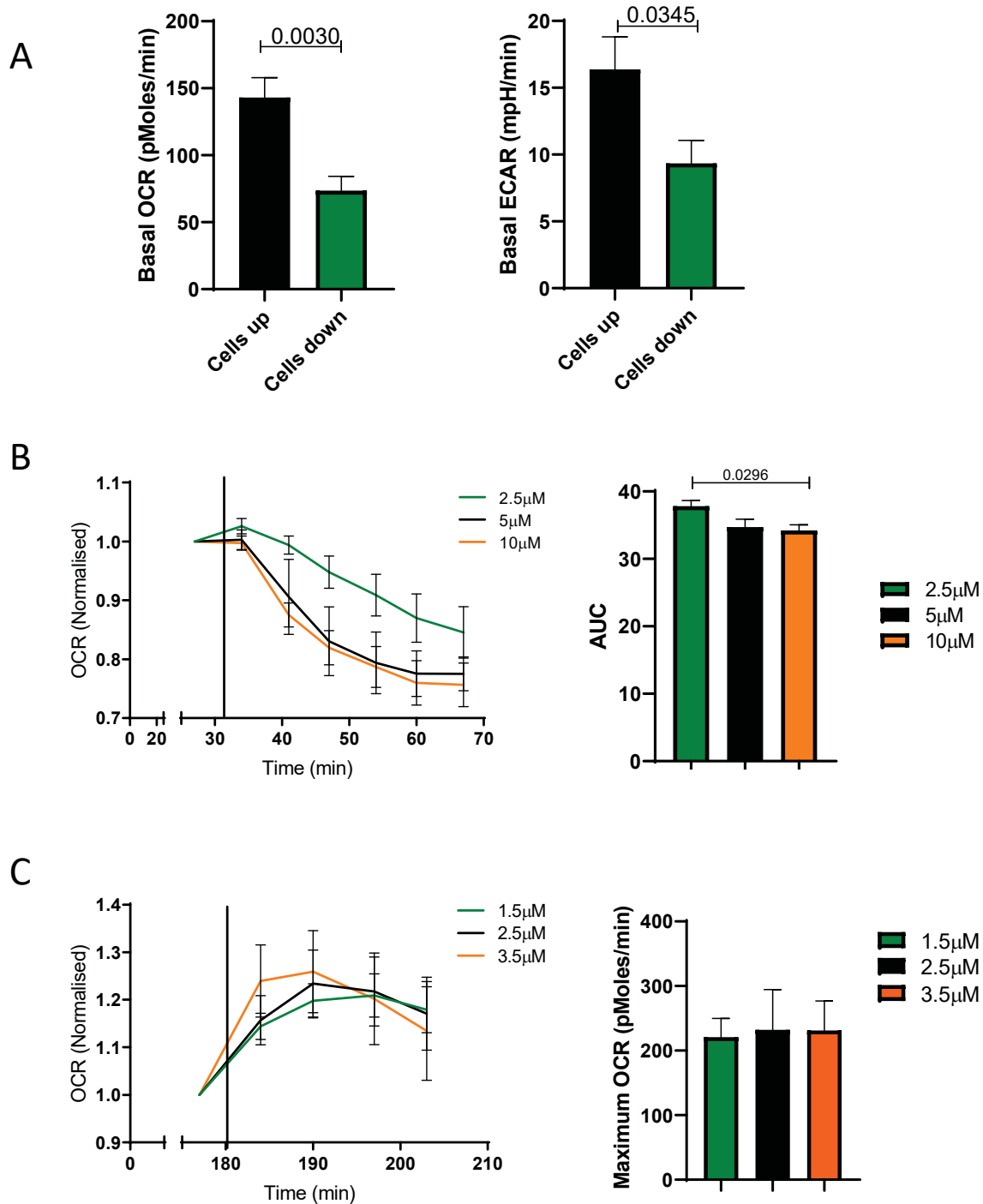
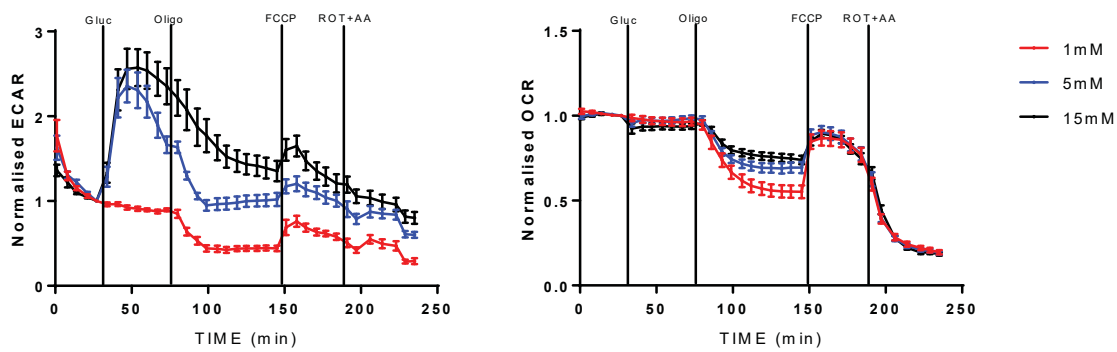
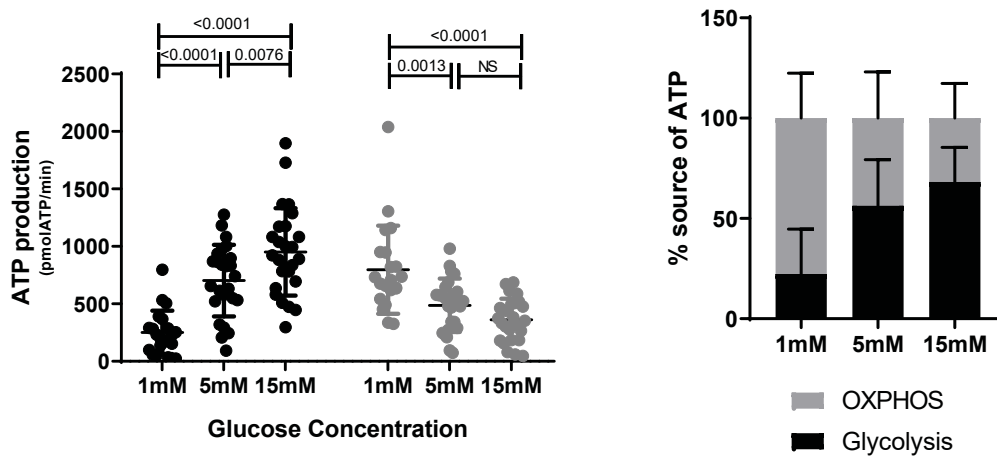


Figure 4 – Metabolic profiling of ALI cells at altered glucose concentration

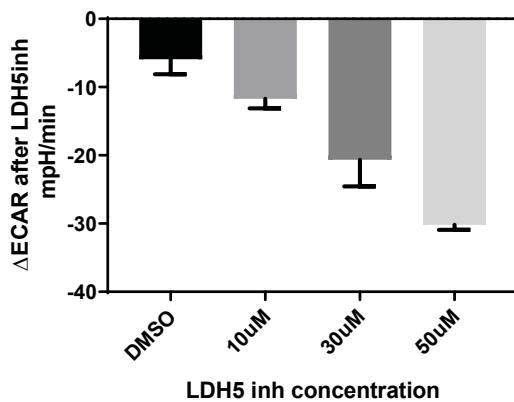
A



B



C



D

